Phase Transition in Confined Water Inside Carbon Nanotubes

Yutaka MANIWA[1,3,*], Hiromichi KATAURA[1], Masatoshi ABE[1], Shinzo SUZUKI[2], Yohji ACHIBA[2], Hiroshi KIRA[1] and Kazuyuki MATSUDA[1]

[1]*Department of Physics, Tokyo Metropolitan University, 1-1 Minami-osawa, Hachioji, Tokyo 192-0397*
[2]*Department of Chemistry, Tokyo Metropolitan University, 1-1 Minami-osawa, Hachioji, Tokyo 192-0397*
[3]*CREST, JST (Japan Science and Technology Corporation)*

(Received August 20, 2002)

In materials confined within nanometer channels in single-walled carbon nanotube (SWNT) bundles, interesting properties which are not observed in bulk materials are expected. In the present paper, we report an X-ray diffraction (XRD) study on water adsorption in SWNT bundles. It was found that a substantial amount of water is absorbed inside SWNTs at room temperature (RT). The desorption-adsorption of water molecules occurred reversibly above RT. We found that the liquid-like water is transformed into a new solid form, *i.e.*, ice nanotubes, at 235 K.

KEYWORDS: water, adsorption, carbon nanotube, structural phase transition, SWNT, ice, ice nanotube

*E-mail address: maniwa@phys.metro-u.ac.jp

Single-walled carbon nanotubes (SWNTs) crystallize into bundles with the closest–packed triangular lattice, where nanometer channels are present inside and outside each SWNT[1-3]. These channels[4-10] can accommodate a large variety of molecules and atoms, and is expected to show interesting properties[11-15] which cannot occur in bulk materials. In particular, water in SWNTs is one of the most interesting molecules because the similar situations can be found in many systems in nature[13-15]. Recent computer simulations have demonstrated novel features in water confined inside SWNTs, such as the formation of polygonal ice nanotubes[13] and unique water conduction[15] through SWNT channels. However, relevant experimental observations have not yet been established. Here, we report a systematic X-ray diffraction (XRD) study[16] on water adsorption in SWNT bundles.

The raw soot of SWNTs used was prepared by laser vaporization of a carbon rod including Ni and Co catalysts[3], and then purified as previously reported[17]. For XRD experiments, the SWNTs were sealed in a quartz capillary with water vapor at room temperature (RT) after removing adsorbed gases[8,18] by heating in vacuum at ~800 K. The average diameter of the SWNTs used was 1.35 to 1.38 nm, close to 1.37 nm of the (10, 10) SWNT. Powder XRD data were collected in the temperature range from 90 K to 570 K using a synchrotron radiation with a wavelength of 0.1000 nm at beam line BL1B in Photon Factory, KEK, Japan. We also studied empty SWNTs[1,2], C_{60}-peapods[7], and double-walled carbon nanotubes[19] (DWNTs) for comparison.

Figure 1 shows examples of XRD patterns taken above 300 K. These patterns can be understood on the basis of the two-dimensional hexagonal lattice[3]. Broadening of each peak is due to the rather small bundle thickness, 10-100 nm in diameter, and the XRD peak profiles are strongly modulated by the tube-form factor, as already extensively discussed[3,8,18]. We first found that the intensity of peak 1 appeared at around Q=4.3 nm^{-1}, indexed as 10 based on the two-dimensional

hexagonal lattice, increases with increase in temperature, and approaches that of the empty SWNT bundles above 470 K, as shown in the inset of Fig. 1. With decreasing temperature to 300 K, the intensity almost returns to its initial value. These data indicate that the desorption or adsorption of water molecules occurs reversibly at around 450 K. In a previous work[8], essentially the same behaviour was observed in SWNT materials in air; this was taken as evidence that air (N_2, O_2, and/or H_2O) molecules can be absorbed inside SWNTs. However the species absorbed were not identified. Water is also known to affect conductivity of the SWNT mat[9,11], but the site of water molecules had not been identified. Here, the present results establish that SWNTs can accommodate water molecules inside.

For further discussions, we simulated the XRD patterns using the three models for the radial density distribution of water inside the SWNT, as shown in Figs. 1(b) and 1(c). The SWNTs were assumed to be a homogeneous charged cylinder forming the closest-packed triangular lattice[3,8,18]. In the simulated profiles (Fig. 1b), one of the main features that vary upon water adsorption is substantial depression of the peak 1 intensity irrespective of the density profile (models 1, 2 and 3), as observed experimentally. This is a tendency opposite to the case where adsorption occurs at the interstitial channels. In such a case, peak 1 intensity must increase. Thus, we are led to the conclusion that water molecules absorb inside SWNTs, as mentioned above. The average number of water molecules inside SWNT was estimated to be roughly 15 water molecules per 1-nm-long SWNT; $C_{11}H_2O$.

A justification of the present simulation is given by results of the comparison of the XRD patterns between the C_{60}-peapods, DWNTs and K-doped C_{60}-peapods. In the cases of C_{60}-peapods and DWNTs, we expect the depression of the peak 1 intensity because the electron density inside SWNTs increases similar to the above models. This tendency was actually observed as shown in Fig. 2. On the other hand, in K-doped

C_{60}-peapods, K ions have to occupy the interstitial channels because there is no sufficient room to accommodate the K ions inside. Thus, in this case, we observed an increase in the peak 1 intensity on K loading (not shown in the figure), as expected from the simulation.

Furthermore, the detailed inspections reveal features depending on the models: In model 1, the intensity of peak 2 (around Q=7.0 nm^{-1}) is smaller than that of the empty SWNTs. On the other hand, model 3 shows the opposite changes to model 1; the intensity of peak 2 increases while those of peaks 3 and 4 (around Q=8.5 and 11.3 nm^{-1}, respectively) decrease. This expectation is justified by a comparison of XRD patterns of DWNTs and C_{60}-peapods with those of the empty SWNT bundles. DWNTs are considered to be a typical example of model 3, while C_{60}-peapods are somewhat closer to the case of model 1. The results in Fig. 2 confirmed the simulated tendency mentioned above, aside from showing that the relative intensities of peaks 2, 3 and 4 are very sensitive to the materials inside SWNTs, *i.e.*, the density profile.

In the case of the water-SWNT system, based on these above considerations, we can conclude that the experimentally observed XRD profile at RT (Fig. 1) is most successfully described by model 2: The changes in the relative intensity of peaks 2, 3 and 4 on water adsorption are well described by model 2. (The shift of the Q-value for the minimum intensity at around Q=8 nm^{-1} also supports this interpretation. The shift is sensitive to the model; for model 1 it shifts to the low-Q region while for model 3 to the high-Q region. Experimentally, because the shift was negligible small, the density profile is most successfully described by model 2.) This distribution (model 2) is interestingly close to that of liquid-like water inferred from computer simulations[13].

Now, we discuss the low-temperature data. Figure 3a shows the typical XRD patterns taken at 255 K and 90 K. Below ~265 K at the sample position, the XRD peaks appear at Q>15 nm^{-1} due to the presence of bulk ice (hexagonal ice). Bulk ice was

formed not only inside but also outside the XRD sample glass tube. Apart from these peaks, we find significant changes in the XRD profile below 235 K. First, the intensity of peak 2 increases while those of 3 and 4 decrease. As already mentioned above, this tendency corresponds to the change from model 2 to model 3 in the water-density profile. To see this more clearly, we also plotted the differential XRD profile at temperatures between 255 K and 90 K in Fig. 3a. The observed features are essentially reproduced by the simulation for models 2 and 3, and their difference (Fig. 3b). Thus, it is known that the liquid-like water is transformed into "water tubes" inside carbon nanotubes. Here, it should be stressed that lattice contraction effects[18] with temperature can be ignored because they show opposite changes to the present observation.

In addition, we found a new peak at Q~22 nm^{-1} below 235 K as shown in Fig. 4a. This peak cannot be assigned to bulk ice (denoted by * in Fig. 4a). The temperature dependence of the intensity of this new peak is shown in Fig. 4b, along with that of peak 2 at Q=7.2 nm^{-1}. Similar variations in the intensities of both peaks imply that they have the same origin, indicating that the confined water inside SWNTs undergoes a structural transition to an ordered state with a tube like density profile. The changes are reversible with temperature and there is no observable difference for decreasing and increasing temperatures. The d-spacing estimated from Q=21.86 nm^{-1} at 90 K is 0.287 nm. The "ice-tube" diameter and its percentage inside SWNTs are estimated to be 0.68±0.05 nm and about 60 %, respectively.

These observations lead us to a structural model for the confined water inside SWNTs below 235 K, as shown in Fig. 4c. This is exactly the ice nanotube proposed by Koga *et. al*[13]. The ice nanotubes satisfy the so-called "bulk ice rule": Each oxygen atom has two donors and two acceptoers of hydrogen in a four-coordinate configuration. The one-dimensional lattice constant 0.287 nm is close to the nearest neighbor oxygen-

oxygen (O-O) bond length in bulk ice of 0.276 nm. The ice-tube diameter of 0.68±0.05 nm is also consistent with that of heptagonal or octagonal ice, which has an O-O bond length of 0.28-0.29 nm.

Although the computer simulations seem to well reproduce the present results, it should be noted that the simulations were performed under axial pressures ranging from 50 to 500 MPa, and the critical temperatures ranged from 200 K to 300 K depending on the tube diameters (1.11-1.34 nm) and the applied pressure. Experimentally, however, the measurements were performed at ambient pressure for SWNTs with an average diameter of 1.35 nm. We should also note that no evidence was observed for water adsorption at the inter tube channels with a diameter of approximately 0.26 nm. Geometrically, these channels could adsorb water molecules. The reason why the adsorption can not occur may be related to different possible hydrogen-bonding networks of water molecules within the confined spaces, as well as different interaction of water molecule with the inside and outside of SWNT wall. These issues, as well as the detailed structures and natures of confined water in SWNTs, are left for future studies.

Authors thank Prof. O. Sakai for useful comments on the manuscript. This work was supported in part by a Grant-in-Aid for Scientific Research on the Priority Area “Fullerenes and Nanotubes” by the Ministry of Education, Science, Sports and Culture of Japan. H. K acknowledges for a Grant-in-Aid for Scientific Research (A), 13304026 by the Ministry of Education, Science, Sports and Culture of Japan.

References

1. S. Iijima and T. Ichihashi: Nature **363** (1993) 603-615.

2. D.S. Bethune, C.H.Kiang, M.S.de Vries, G.Gorman, R.Savoy, J.Vasquez, and R. Beyers: Nature **363** (1993) 605-607.

3. A. Thess, R. Lee, P. Nikolaev, H. Dai, P. Petit, J. Robert, C. Xu, Y.H. Lee, S.G. Kim, A.G. Rinzler, D.T. Colbert, G.E. Scuseria, D. Tomanek, J.E. Fischer, and R.E. Smally: Science **273** (1996) 483-487.

4. M.R. Pederson and J.Q. Broughton: Phys. Rev. Lett. **69** (1992) 2689-2692.

5. R.S. Lee, H.J. Kim, J.E. Fischer, A. Thess, and R.E. Smalley: Nature **388** (1997) 255-257.

6. X. Fan, E. C. Dickey, P. C. Eklund, K. A. Williams, L. Grigorian, R. Buczko, S. T. Pantelides, and S. J. Pennycook: Phys. Rev. Lett. **84** (2000) 4621-4624.

7. B.W. Smith, M. Monthioux and D.E. Luzzi: Nature **396** (1998) 323-324.

8. Y. Maniwa, Y. Kumazawa, Y. Saito, H. Tou, H. Kataura, H. Ishii, S. Suzuki, Y. Achiba, A. Fujiwara and H. Suematsu: Jpn. J. Appl. Phys. **38** (1999) L668-670.

9. Y. Maniwa, Y. Kumazawa, Y. Saito, H. Tou, H. Kataura, H. Ishii, S. Suzuki, Y. Achiba, A. Fujiwara and H. Suematsu,: Mol. Cryst. and Liq. Cryst. **340** (2000) 671-676.

10. A. Zahab, L. Spina, P. Poncharal, and C. Marlière: Phys. Rev. B **62** (2000) 10000-10003.

11. M.M. Calbi, M.W. Cole,S.M. Gatica, M.J. Bojan, G. Stan: Rev. Mod. Phys. **73** (2001) 857-865.

12. J. Marti & Gordillo: Phys. Rev. E **64** (2001) 021504-1-6.

13. K. Koga, G.T. Gao, H. Tanaka and X.C. Zeng: Nature **412** (2001) 802-805.

14. M.S.P. Sanson and P.C. Biggin: Nature **414** (2001) 156-157.

15. G. Hummer, J.C. Rasaiah and J.P. Noworyta: Nature **414** (2001) 188-190.

16. It has been well known that powder XRD is one of powerful techniques to determine the detailed structure of fullerene and related materials (M. Takata, *et. al*.: Nature **377** (1995) 46-49). In the field of carbon nanotubes, however, the use of powder XRD has been rather limited because of difficulty in preparation of single-phase materials and their small crystallized domains. However, recent development in the preparation method makes it possible to deduce new insights into the structure of carbon nanotubes. In the present study, we used the best-quality polycrystalline SWNTs within our knowledge.

17. H. Kataura, Y. Maniwa, T. Kodama, K. Kikuchi, H. Hirahara, K. Suenaga, S. Iijima, S. Suzuki, Y. Achiba and W. Kraetschmer: Synthetic Metals **121** (2001) 1195-1196.

18. Y. Maniwa, R. Fujiwara, H. Kira, H. Tou, H. Kataura, S. Suzuki, Y. Achiba, E. Nishibori, M. Takata, M. Sakata, A. Fujiwara and H. Suematsu: Phys. Rev. B **64** (2001) 241402(R)-1-3.

19. S. Bandow, M. Takizawa, H. Hirahara, M. Yudasaka and S. Iijima: Chem. Phys. Lett.*:* Chem. Phys. Lett. **337** (2001) 48.

20. H. Kataura, Y. Maniwa, M. Abe, A. Fujiwara, T. Kodama, K. Kikuchi, H. Imahori, Y. Misaki, S. Suzuki, and Y. Achiba: Appl. Phys. **A 74** (2002) 349-354.

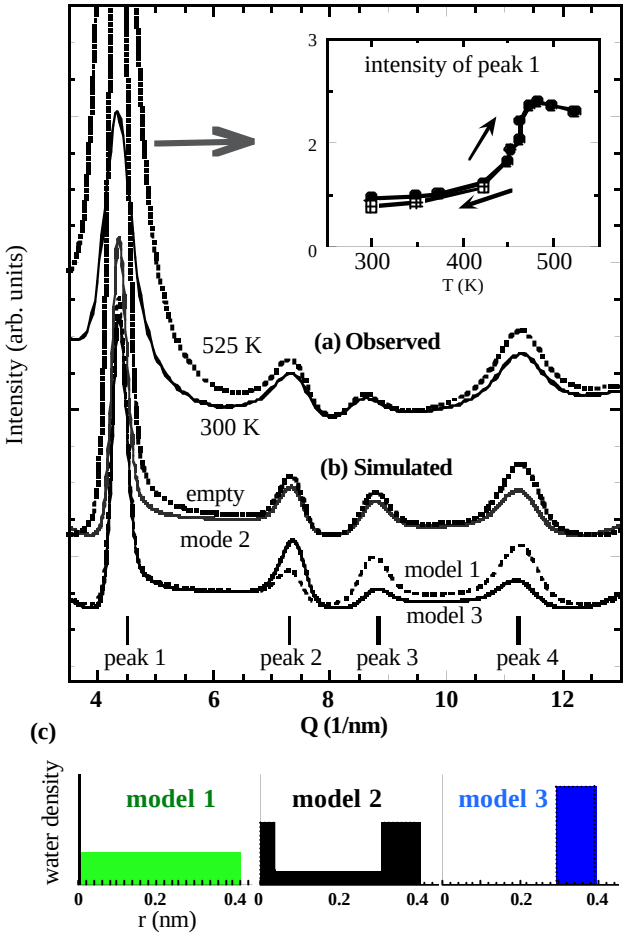

Figure 1. X-ray diffraction (XRD) profiles of water-exposed SWNT bundles. (a) Observed profiles taken at 525 K and 300 K. (b) Simulated XRD profiles for empty SWNT bundles (dotted line), water-encapsulated SWNT bundles for models 1, 2 and 3. (c) Radial density distribution of water molecules for models 1, 2 and 3. "r" denotes the distance from the center of the tube. Q is the amplitude of the scattering vector; $Q=4\pi\sin q/l$ with the wave length l and scattering angle $2q$. The inset is the temperature dependence of the intensity of peak 1 that appeared around $Q=4.3$ nm^{-1}.

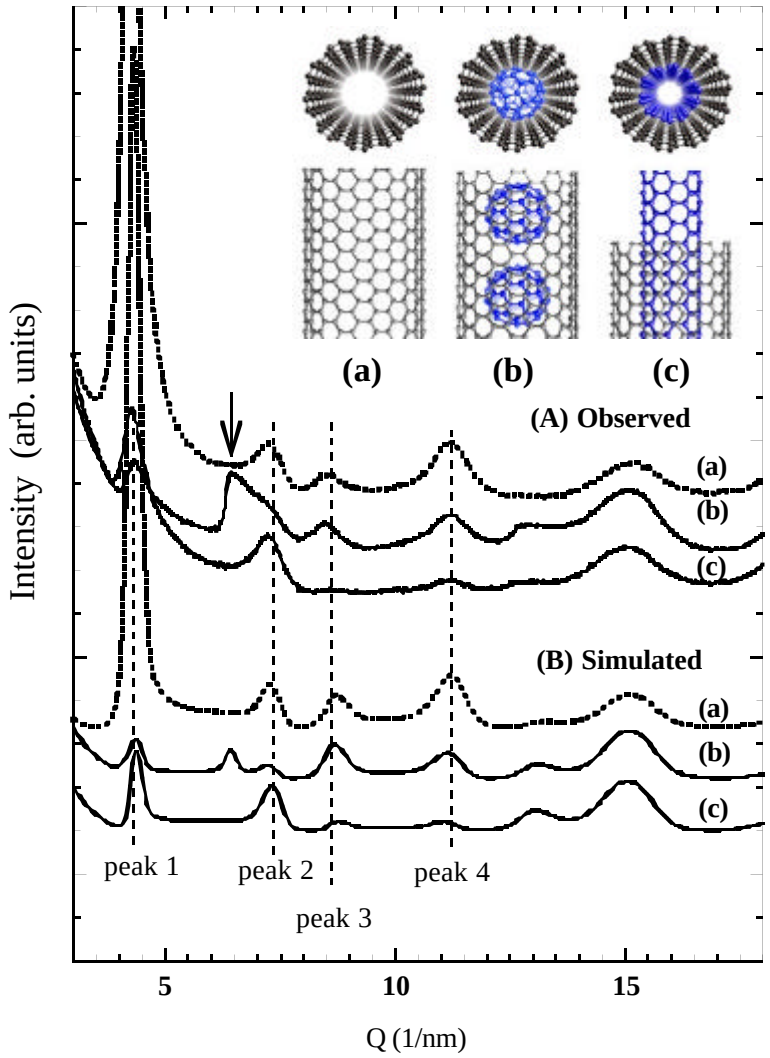

Figure 2. XRD profiles for empty SWNT bundles (a), C_{60}-peapod bundles (b), and DWNT bundles (c). (A) Experimentally observed patterns taken at room temperature. (B) Simulated XRD patterns in the uniformly charge distribution model. In C_{60}-peapod, the arrow shows the diffracted peak from the one-dimensional array of C_{60} molecules inside SWNTs.

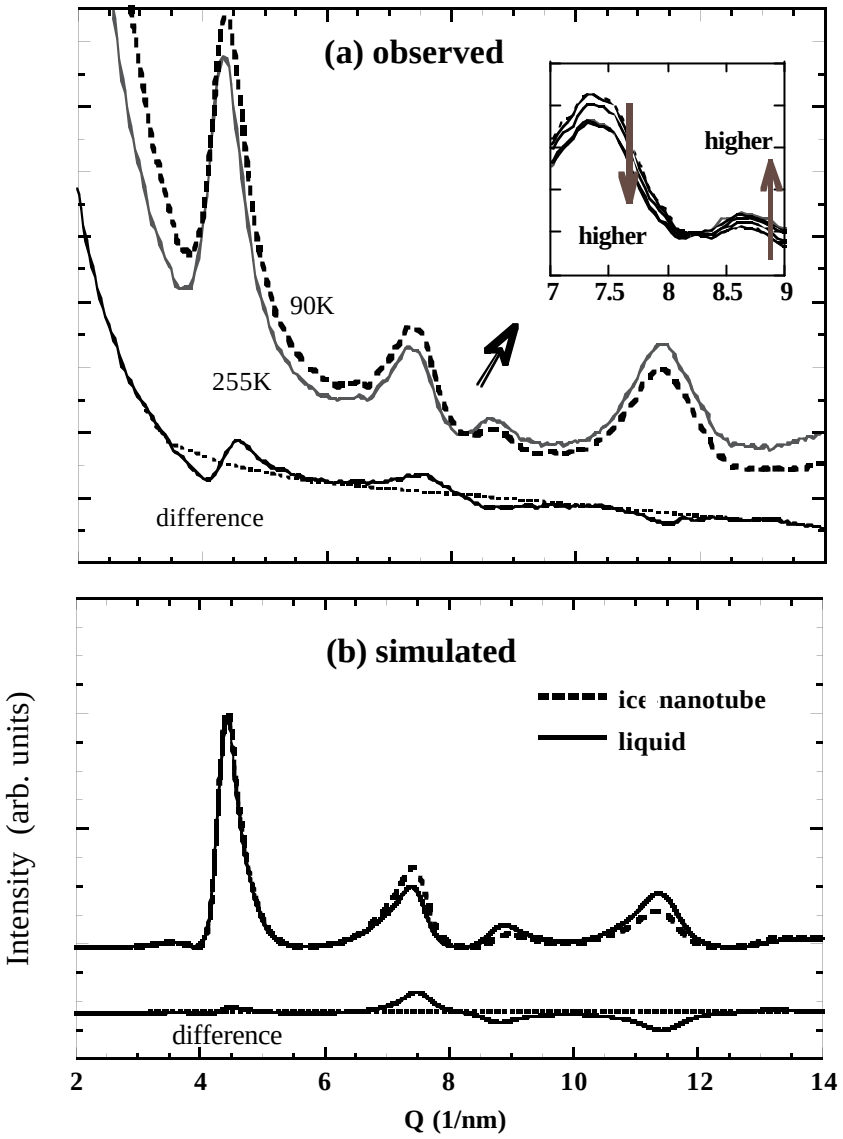

Figure 3. (a) XRD profiles in water-exposed SWNT bundles taken at 255 K (solid line) and 90 K (dotted line). The difference is also shown. (b) Simulated XRD profiles in SWNT bundles encapsulating liquid water described by model 2 (solid line) and solid ice nanotube described by model 3 (dotted line). The difference is shown below. (The sample is different from that shown in Fig. 1.)

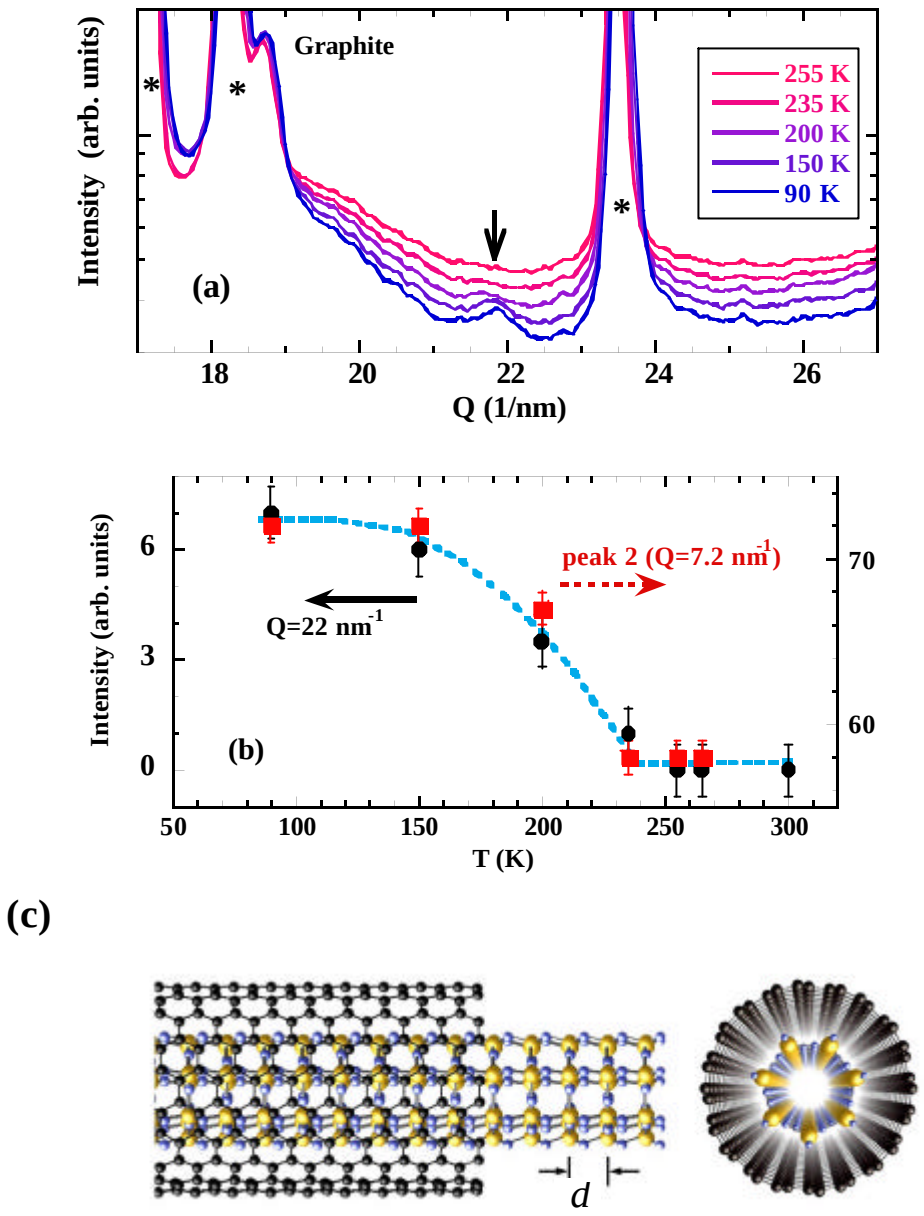

Figure 4. (a) Temperature dependence of XRD profiles in water-exposed SWNT bundles. Stars (*) denote peaks due to bulk ice. (b) Temperature dependence of the intensity of the peak around Q=22 nm^{-1} shown by the arrow in Fig. 4a, along with that of peak 2 at around Q=7.2 nm^{-1}. The background intensity due to the presence of a quartz capillary was subtracted. (c) The proposed structure of the ice nanotube inside a SWNT. The estimated d-spacing is 0.287 nm at 90 K.